ChemComm

COMMUNICATION

View Article Online
View Journal | View Issue

Cite this: *Chem. Commun.*, 2025, **61**, 17400

Received 20th August 2025,
Accepted 3rd October 2025

DOI: 10.1039/d5cc04806k

rsc.li/chemcomm

AIE Ir(III) complex conjugated with biotin as a photosensitizer for enhanced photodynamic anticancer therapy

Zihan Wu,†[a] Runlin Wang,†[a] Chunguang Shi,[a] Dongxia Zhu *[a] and Martin R. Bryce *[b]

The first aggregation induced emission (AIE) Ir(III) complex bearing a biotin-functionalized ligand, Ir-Bio, is reported. Ir-Bio generates type I and type II reactive oxygen species and has an excellent photodynamic therapy effect in cancer cells.

Photodynamic therapy (PDT) is a non-invasive treatment that uses photosensitizers (PSs), light and oxygen (O_2) to selectively combat malignant tumors, vascular diseases and microbial infections.[1–3] PSs can operate through two main mechanisms: type I and type II. The type II mechanism involves sensitizing singlet oxygen ($^1O_2$) through an energy-transfer process from the excited triplet state of the PS to molecular oxygen in the ground state.[4,5] Regrettably, the highly hypoxic tumor microenvironment significantly limits the effect of type II PDT against tumors.[6] The type I PDT mechanism is based on electron transfer reactions that generate a variety of reactive oxygen species (ROS), such as superoxide ($^{\bullet}O_2^-$) and hydroxyl ($^{\bullet}OH$) radicals.[7,8] Type I PSs decrease reliance on O_2 and demonstrate significant promise in addressing tumor hypoxia.[9]

One of the major challenges of PDT technology is how to obtain sufficient quantities of the PSs in the target tissue for effective treatment.[10] There remains an urgent need for PSs with specific targeting ability. Many Ir(III) complexes have attracted attention as candidate drugs for anticancer therapy due to their unique physiological properties and favorable photophysical attributes, including easy synthesis, structural modifications, strong photostability, and so on.[11–13] Iridium metal centers can be coordinated with different bidentate ligands through rational design strategies. Therefore, the auxiliary ligands and cyclometalated ligands can be tuned to have different biological functions to enrich the role of Ir(III) complexes in biological research and therapeutic applications. When the ligands are modified with targeting molecules, the Ir(III) complex will accumulate in large quantities in cancer cells, thus improving the antitumor properties. Cancer cells frequently exhibit high levels of tumor-specific receptors, including biotin receptors that facilitate accelerated growth, proliferation, and survival of the cells.[14–19] Purushothaman *et al.*[20] conjugated biotin as a targeting agent to the chlorophyll derivative TPP, which achieved selective targeting of the breast cancer cell line MCF-7. However, TPP derivatives may suffer aggregation-caused quenching (ACQ) of emission in aqueous media, reducing the ROS production. Thus, leveraging the excellent tumor-targeting ability of biotin and easy modifications of Ir(III) complexes should be an effective strategy to enhance PDT outcomes. However, to date the modification of Ir(III) complexes with biotin for this purpose has not been reported.

Most PSs for PDT are based on organic dyes, including boron dipyrromethene (BODIPY), porphyrin, and their derivatives which have a large planar π-electron system which favours ACQ.[21–23] The opposite phenomenon, namely aggregation-induced emission (AIE), can enhance fluorescence and ROS generation in an aggregate state through restriction of intramolecular motion (RIM) which prohibits the dissipation of energy.[24] PSs with AIE characteristics overcome the ACQ problem of traditional PSs and have the following advantages: (i) the intersystem crossing (ISC) ability of excited states is significantly improved, (ii) the luminescent quantum efficiency is enhanced, (iii) there is high ROS generation. To date, a few AIE Ir(III) complexes have been reported as PSs, and obtaining AIE Ir(III) complexes as antitumor agents remains a challenge.[25,26]

In the current work, biotin is linked to the auxiliary ligand to construct the neutral AIE Ir(III) complex **Ir-Bio** with the following desirable features: (i) the ability to generate type I ROS is obtained, (ii) the generation of type II ROS is greatly improved, (iii) the complex effectively accumulates in tumor cells. The PSs **Ir1** (Fig. 1(A)) and **Ir-Bio** (Scheme 1) were obtained by a simple Schiff base reaction in high yields. With the introduction of the

[a] *Key Laboratory of Nanobiosensing and Nanobioanalysis at Universities of Jilin Province, Department of Chemistry, Northeast Normal University, 5268 Renmin Street, Changchun, Jilin Province 130024, P. R. China. E-mail: zhudx047@nenu.edu.cn*

[b] *Department of Chemistry, Durham University, Durham, DH1 3LE, UK. E-mail: m.r.bryce@durham.ac.uk*

† The authors contributed equally to the preparation of this work.

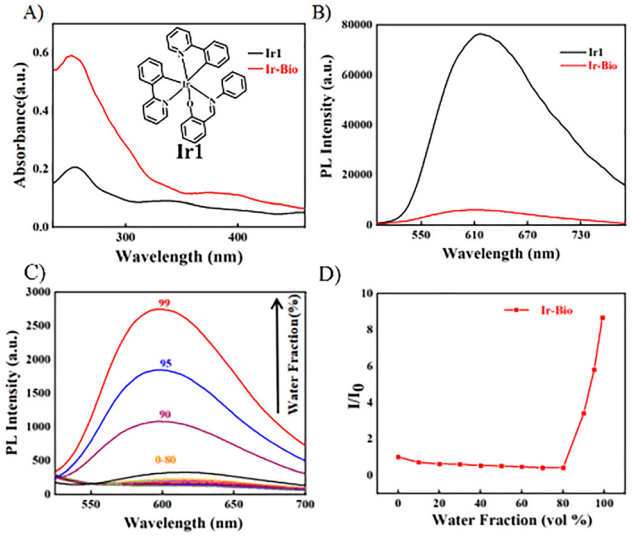

Fig. 1 (A) Ultraviolet (UV)-vis absorption spectra of **Ir1**/**Ir-Bio** (10^{-5} M) in CH_3CN/H_2O (v : v = 1 : 9); (B) fluorescence emission spectra, λ_{ex} = 400 nm; (C) fluorescence emission spectra of **Ir-Bio** in CH_3CN/H_2O mixed solution (10^{-5} M), λ_{ex} = 400 nm; (D) the change of the emission intensity of **Ir-Bio** in CH_3CN/H_2O with the change of the water concentration.

biotin-assisted ligand, the light absorption and singlet oxygen production capacity of **Ir-Bio** are significantly enhanced compared to **Ir1**. **Ir-Bio** readily accumulates in cells and has high ROS production capacity, which effectively improves the PDT antitumor effect. The work provides a new perspective to address the oxygen deficiency limitation of PSs in PDT, and to improve the uptake of PSs into cancer cells.

The synthetic routes to the ligands L1, L2, and the complexes **Ir1** and **Ir-Bio** (Schemes S1–S5) and corresponding characterization data are provided in the SI with ^{1}H NMR and mass spectra (Fig. S1–S6). The UV-Vis absorption spectra of **Ir1** and **Ir-Bio** at room temperature are shown in Fig. 1(A). Both complexes show strong absorption peaks in the ultraviolet region, and the bands in the range of 250–350 nm are attributed to the π → π* transition centered on the ligands. The relatively weak absorption bands in the visible region can be attributed to metal-to-ligand charge transfer transitions, spin-permitted ligand-to-ligand charge transfer transitions, spin-barred metal-to-ligand charge transfer transitions, and spin-barred ligand-to-ligand charge transfer transitions. As shown in Table S1, the absorptive capacity of **Ir-Bio** (ε 58 571 and 12 063 m^{-1} cm^{-1}) was significantly increased compared to **Ir1** due to the introduction of biotin, indicating high efficiency in photon absorption and utilization. The emission spectra of **Ir1** and **Ir-Bio** were similar, with λ_{max} at 610 nm (Fig. 1(B)).

The AIE properties of **Ir1** and **Ir-Bio** were investigated in CH_3CN–H_2O mixtures, where the water content varied from 0 to 99%. As shown in Fig. 1(C), (D) and Fig. S7, **Ir1** and **Ir-Bio** barely emit in pure CH_3CN due to the non-radiative transition process enhanced by molecular vibrations and rotations. As the water content increased to 95%, **Ir1** shows a strong red emission (Fig. S7). **Ir-Bio** showed strongest red emission when the water content increased to 99%. These results establish that **Ir1** and **Ir-Bio** have typical AIE characteristics which will be beneficial to enhance ROS production and therefore improve the effect of PDT.

Efficient $^1O_2$ generation is very important for PSs to improve the PDT effect. The $^1O_2$ production of **Ir1** and **Ir-Bio** in DMSO : H_2O (v : v = 1 : 99) was evaluated by monitoring the absorbance changes of indocyanine green (ICG) at 790 nm. For ICG alone, the absorption intensity basically did not change during 210 s of illumination (Fig. 2(A)). Also, the spectra of ICG in the presence of **Ir1** or **Ir-Bio** showed little change without light (Fig. S8). In the cell experiments, PSs need to be irradiated for a relatively long time, and PSs with good light stability are therefore advantageous for PDT. The UV-vis absorption spectra of **Ir1** and **Ir-Bio** did not change during 210 s of illumination which proved their good photostability (Fig. S9). When irradiated with a 405 nm LED lamp for 210 s, the ICG absorption at 790 nm significantly decreased (by > 80%) in the presence of **Ir-Bio** compared with **Ir1** (only about 20%) (Fig. 2(B)–(D)). This data establishes the excellent $^1O_2$ generation ability of **Ir-Bio**. As shown in Fig. 2(E), these data for **Ir1** and **Ir-Bio** conform to the first-order kinetic equation. The higher the slope of the straight line, the stronger the $^1O_2$ generation capacity. The **Ir-Bio** slope (0.00757) is 8.5 times that of **Ir1** (0.000888). Using Rose Bengal (RB singlet oxygen production efficiency of 73%) as a reference, the $^1O_2$ quantum yields of **Ir1** and **Ir-Bio** were 17% and 88%, respectively.

Most PSs rely on oxygen to produce singlet oxygen, which is cytotoxic, to achieve cell damage. The oxygen consumption during PDT will further aggravate the oxygen deficiency in the tumor. Therefore, type I PSs that can produce superoxide anion radicals ($^{\bullet}O_2^-$) have a broad application in PDT. As shown in Fig. 2(F), **Ir1** (0.1 mM) and 2,2-dimethyl-1-oxido-3,4-dihydropyrrol-1-ium (DMPO as a spin-trapping agent for free radicals) (100 mM) showed no EPR signal in DMSO solution under either dark or light conditions, indicating that **Ir1** could not produce superoxide anion radicals. In the dark, **Ir-Bio** (0.1 mM) and DMPO (100 mM) also did not give any EPR signal. However, when the **Ir-Bio** and DMPO solution was illuminated, the characteristic superoxide anion radical signal was generated. Therefore, **Ir-Bio** can realize a type I PDT process and effectively overcome the limitation of

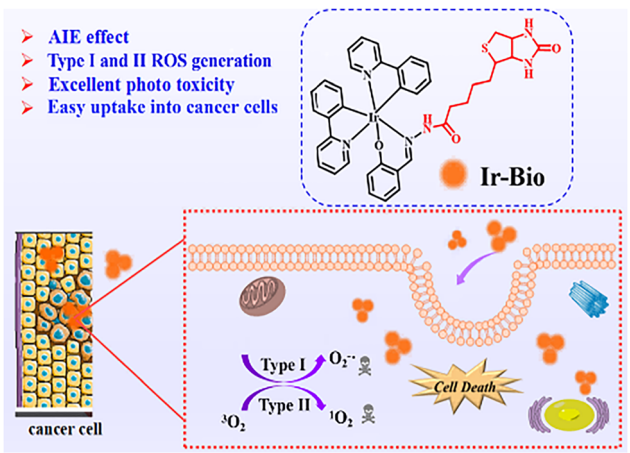

Scheme 1 Structural formula of **Ir-Bio** and its PDT process.

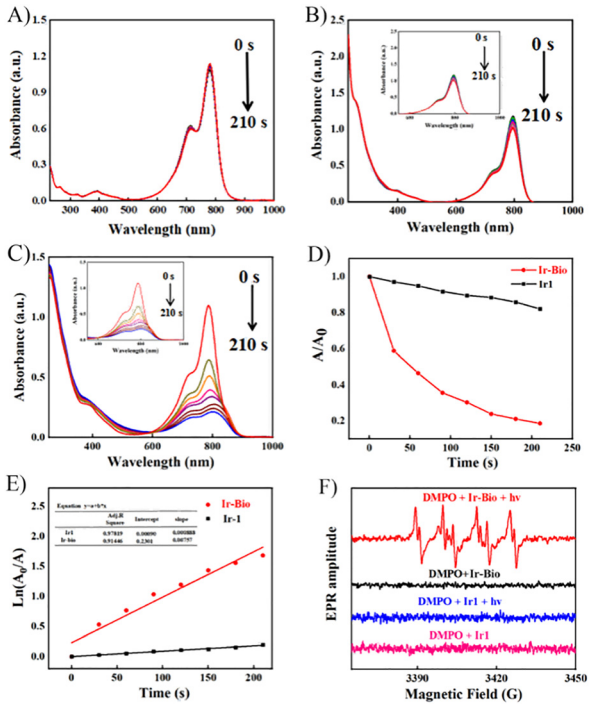

Fig. 2 (A) UV absorption spectra of ICG at different illumination times (405 nm, 20 mW cm^{-2}); (B) ICG + **Ir1** + light; (C) ICG + **Ir-Bio** + light; (D) the attenuation curve of ICG at 790 nm when **Ir1** or **Ir-Bio** (18 μM) is present under different illumination times, data in DMSO : H_2O (v : v = 1 : 99); (E) $^1O_2$ kinetic generation curve of **Ir1**/**Ir-Bio**; (F) EPR signals of **Ir1** and **Ir-Bio** (0.1 mM) and DMPO (100 mM) under light and dark conditions in DMSO.

photosensitizer oxygen deficiency in PDT, which opens a new platform for the application of transition metal Ir(III) complex PSs in PDT. In DMSO : H_2O solution (1 : 99 v : v) **Ir1**/DMPO and **Ir-Bio**/DMPO gave no $^{\bullet}OH$ EPR signal under light (405 nm, 20 mW cm^{-1}) or dark, indicating that $^{\bullet}OH$ is not generated in aqueous conditions.

Since **Ir1** and **Ir-Bio** showed excellent ROS production ability in solution, we studied their PDT *in vitro* by 3-(4,5-dimethylthiazol-2-yl)-2,5-diphenyltetrazolium bromide (MTT) assay. As shown in Fig. 3, HeLa cell survival exceeded 80% in dark conditions, even with photosensitizer concentrations up to 50 μM, indicating relatively low dark toxicity of **Ir1** and **Ir-Bio**. However, **Ir1** and **Ir-Bio** showed concentration-dependent phototoxicity with increasing concentration when irradiated by an LED lamp with emission wavelength of 405 nm. When **Ir1** concentration reached 50 μM, the cell survival rate was only about 20%. When the **Ir-Bio** concentration was only 25 μM, the cell survival rate was already reduced to less than 10%. Since **Ir1** does not produce superoxide anions, both the **Ir1** dark group and the **Ir1** light group did not exhibit significant cytotoxicity under hypoxic conditions. Therefore, the phototoxicity of **Ir1** under normoxic conditions should be primarily attributed to the type II photodynamic process. The cell survival rate in the irradiated group with **Ir-Bio** at concentration of 50 μM was less than 40%. This result proved that **Ir-Bio** could still effectively kill HeLa cells under hypoxic conditions (Fig. S10). Therefore, **Ir-Bio** has better potential than **Ir1** as a PS for cancer treatment.

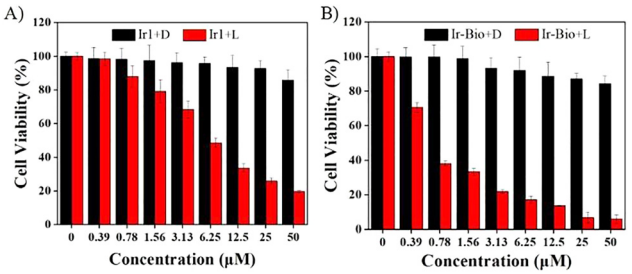

Fig. 3 Survival rate of (A) **Ir1** and (B) **Ir-Bio**-pretreated HeLa cells under dark (D) and illuminated (L) conditions (405 nm, 20 mW cm^{-2}).

We further detected and verified ROS production in HeLa cells by using the indicator 2′,7′-dichlorofluorescein diacetate (DCFH-DA). As shown in Fig. 4(A), (B) and Fig. S11 in the presence of the PSs **Ir1** and **Ir-Bio**, the intracellular cells showed obvious green fluorescence after light exposure, indicating that DCFH-DA was oxidized to green-emitting DCF by ROS produced by the intracellular photosensitizers. According to the above data **Ir1** and **Ir-Bio** photosensitizers can effectively produce ROS in cells under light.

To observe the live and dead states of cells after the PDT treatment, calcein-AM (live cells, green fluorescence) and propidium iodide (PI) (dead cells, red fluorescence) were co-stained with HeLa cells to determine the cell death through different fluorescence changes. As shown in Fig. 4(C), (D) and Fig. S12, in the absence of the photosensitizers, green fluorescence was emitted in the cells, and basically no red fluorescence was observed, indicating good cell growth. However, upon illumination at λ_{em} 405 nm, the cells showed strong red fluorescence, and basically no green fluorescence. The HeLa cells co-incubated with **Ir-Bio** emitted stronger red fluorescence which indicated that **Ir-Bio** was more enriched in HeLa cells to show better phototoxicity due to the presence of the biotin unit. The results of the live/dead cell staining are consistent with the MTT assay, indicating that **Ir-Bio** is highly enriched and has

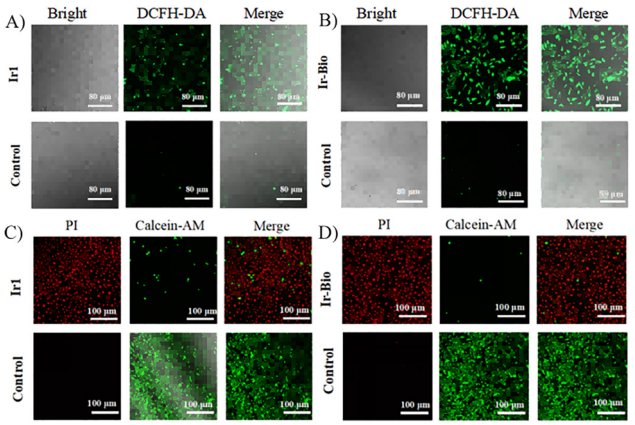

Fig. 4 The intercellular $^1O_2$ capacity was evaluated by DCFH-DA fluorescence intensity after (A) **Ir1** and (B) **Ir-Bio** under darkness and illumination (405 nm, 20 mW cm^{-2}); (C) **Ir1** was used; (D) fluorescent images of HeLa cells incubated with **Ir-Bio** (50 μM).

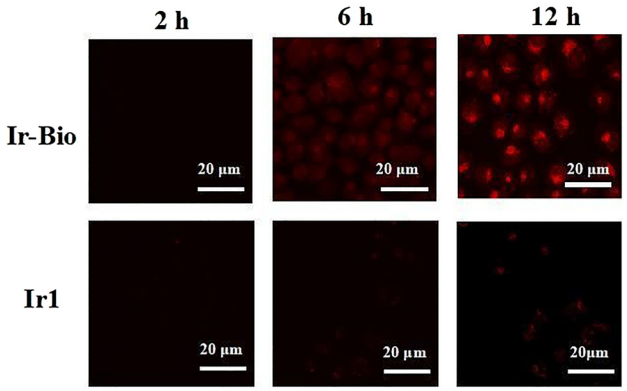

Fig. 5 CLSM images of HeLa cells incubated with **Ir1** or **Ir-Bio** for 2 h, 6 h and 12 h.

high ROS production ability in cancer cells, which provides a new molecular strategy to solve the difficulty of transition metal complex photosensitivities in hypoxic PDT.

The uptake of PSs in cells is an important factor affecting the efficacy of tumor therapy. As shown in Fig. 5 and Fig. S13, both **Ir1** and **Ir-Bio** showed time-dependent enhancement of red fluorescence in HeLa cells through confocal laser scanning microscopy (CLSM), indicating that the uptake capacity of both PSs increased gradually over time. In addition, compared with **Ir1**, it was obvious that HeLa cells incubated with **Ir-Bio** emitted much stronger red fluorescence for the same incubation time. Furthermore, the uptake ability of A549 cells for the two photosensitizers (**Ir1** and **Ir-Bio**) was measured (Fig. S14 and S15).

After 6 hours of co-incubation with **Ir-Bio**, red fluorescence was emitted within the cells indicating that **Ir-Bio** was effectively internalized by the cells due to stronger uptake of biotin-conjugated ligands, compared with **Ir1**, which would contribute to better PDT killing of cancer cells by **Ir-Bio**. Furthermore, to verify that the uptake is receptor-specifically mediated, we performed a binding assay by incubating HeLa cells with free biotin. After incubating with free biotin for one hour, **Ir-Bio** was added for further incubation. It is notable that no red fluorescence was observed even after 6 hours of co-incubation. This is attributed to the complete binding of the free biotin to the over-expressed biotin receptor on the surface of the HLla cells (Fig. S16 and S17).

In summary, the significance of this work stems from the rational design of an Ir(III) complex bearing biotin functionality on the ancillary ligand. Specifically: (i) **Ir-Bio** has an excellent AIE effect; (ii) **Ir-Bio** achieves type I and type II PDT, and (III) the biotin ligand is beneficial to internalization of the Ir(III) complex by HeLa cells. Overall, this work provides an effective and versatile strategy for improving the PDT effect of Ir(III) complex photosensitizers under hypoxic conditions. Future work will address ligand design for obtaining longer wavelength absorption in **Ir-Bio** complex PSs.

This work was supported by NSFC (no. 52473167), the Key Scientific and Technological Project of Jilin Province (20240402036GH), the Development and Reform Commission of Jilin Province (2024C017-4). M. R. B. thanks EPSRC (UK) grant EP/L02621X/1 for funding.

Conflicts of interest

There are no conflicts to declare.

Data availability

The data associated with this article are available in the manuscript and supplementary information (SI). Supplementary information: experimental details, supporting figures and tables. See DOI: **https://doi.org/10.1039/d5cc04806k**.

Notes and references

1 Z. Zhou, J. Song, L. Nie and X. Chen, *Chem. Soc. Rev.*, 2016, **45**, 6597–6626.
2 X. Zhong, X. Wang, J. Li, J. Hu, L. Cheng and X. Yang, *Coord. Chem. Rev.*, 2021, **437**, 213828.
3 Y. Wan, L.-H. Fu, C. Li, J. Lin and P. Huang, *Adv. Mater.*, 2021, **33**, 2103978.
4 G. Li, M. Wu, Y. Xu, Q. Wang, J. Liu, X. Zhou, H. Ji, Q. Tang, X. Gu, S. Liu, Y. Qin, L. Wu and Q. Zhao, *Coord. Chem. Rev.*, 2023, **478**, 214979.
5 D. Zhu, Y. Duo, M. Suo, Y. Zhao, L. Xia, Z. Zheng, Y. Li and B. Z. Tang, *Angew. Chem., Int. Ed.*, 2020, **59**, 13836.
6 J.-N. Liu, W. Bu and J. Shi, *Chem. Rev.*, 2017, **117**, 6160.
7 K. Chen, P. He, Z. Wang and B. Z. Tang, *ACS Nano*, 2021, **15**, 7735.
8 R. Lin, J. Liu, W. Xu, Z. Liu, X. He, C. Zheng, M. Kang, X. Li, Z. Zhang, H. T. Feng, J. W. Y. Lam, D. Wang, M. Chen and B. Z. Tang, *Adv. Mater.*, 2023, **35**, e2303212.
9 M. Li, J. Xia, R. Tian, J. Wang, J. Fan, J. Du, S. Long, X. Song, J. W. Foley and X. Peng, *J. Am. Chem. Soc.*, 2018, **140**, 14851.
10 J. Li, L. Zeng, K. Xiong, T. W. Rees, C. Jin, W. Wu, Y. Chen, L. Jia and H. Chao, *Chem. Commun.*, 2019, **55**, 10972–10975.
11 D.-Y. Zhang, Y. Zheng, H. Zhang, J.-H. Sun, C.-P. Tan, L. He, W. Zhang, L.-N. Ji and Z.-W. Mao, *Adv. Sci.*, 2018, **5**, 1800581.
12 L. Zhang, Y. Li, W. Che, D. Zhu, G. Li, Z. Xie, N. Song, S. Liu, B. Z. Tang, X. Liu, Z. Su and M. R. Bryce, *Adv. Sci.*, 2019, **6**, 1802050.
13 P. Zhang, C. K. Chiu, H. Huang, Y. P. Lam, A. Habtemariam, T. Malcomson, M. J. Paterson, G. J. Clarkson, P. B. O'Connor, H. Chao and P. J. Sadler, *Angew. Chem., Int. Ed.*, 2017, **56**, 14898.
14 M. Li, J. Xia, R. Tian, J. Wang, J. Fan, J. Du, S. Long, X. Song, J. W. Foley and X. Peng, *J. Am. Chem. Soc.*, 2018, **140**, 14851–14859.
15 K. H. Gebremedhin, M. Li, F. Gao, B. Gurram, J. Fan, J. Wang, Y. Li and X. Peng, *Dyes Pigm.*, 2019, **170**, 107617.
16 D. Li, X.-Z. Wang, L.-F. Yang, S.-C. Li, Q.-Y. Hu, X. Li, B.-Y. Zheng, M.-R. Ke and J.-D. Huang, *ACS Appl. Mater. Interfaces*, 2019, **11**, 36435–36443.
17 X. Pei, F. Huo, Y. Yue, T. Chen and C. Yin, *Sens. Actuators, B*, 2020, **304**, 127431.
18 K. Li, L. Qiu, Q. Liu, G. Lv, X. Zhao, S. Wang and J. Lin, *J. Photochem. Photobiol., B*, 2017, **174**, 243–250.
19 C. Wang, Y. Xiu, Y. Zhang, Y. Wang, J. Xu, W. Yu and D. Xing, *Nanoscale*, 2025, **17**, 1812–1873.
20 B. Purushothaman, J. Choi, S. Park, J. Lee, A. A. S. Samson, S. Hong and J. M. Song, *J. Mater. Chem. B*, 2019, **7**, 65.
21 H. He, S. Ji, Y. He, A. Zhu, Y. Zou, Y. Deng, H. Ke, H. Yang, Y. Zhao, Z. Guo and H. Chen, *Adv. Mater.*, 2017, **29**, 1606690.
22 B. Yu, S. Goel, D. Ni, P. A. Ellison, C. M. Siamof, D. Jiang, L. Cheng, L. Kang, F. Yu, Z. Liu, T. E. Barnhart, Q. He, H. Zhang and W. Cai, *Adv. Mater.*, 2018, **30**, 1704934.
23 B. Yu, H. Wei, Q. He, C. A. Ferreira, C. J. Kutyreff, D. Ni, Z. T. Rosenkrans, L. Cheng, F. Yu, J. W. Engle, X. Lan and W. B. Cai, *Angew. Chem., Int. Ed.*, 2018, **57**, 218.
24 L. Liu, C. Li, J. Gong, Y. Zhang, W. Ji, L. Feng, G. Jiang, J. Wang and B. Tang, *Angew. Chem., Int. Ed.*, 2023, **62**, e202307776.
25 L. Zhang, Y. Li, W. Che, D. Zhu, G. Li, Z. Xie, N. Song, S. Liu, B. Tang, X. Liu, Z. Su and M. R. Bryce, *Adv. Sci.*, 2019, **6**, 1802050.
26 S. Liu, Y. Pei, Y. Sun, Z. Wang, H. Chen, D. Zhu, M. R. Bryce, B. Tang and Y. Chang, *Aggregate*, 2024, **5**, e547.